

Design Optimization of Axial Flow Compressor Blades with Three-Dimensional Navier-Stokes Solver

Sang-Yun Lee, Kwang-Yong Kim*

School of Mechanical, Aerospace and Automation Engineering, Inha University

Numerical optimization techniques combined with a three-dimensional thin-layer Navier-Stokes solver are presented to find an optimum shape of a stator blade in an axial compressor through calculations of single stage rotor-stator flow. Governing differential equations are discretized using an explicit finite difference method and solved by a multi-stage Runge-Kutta scheme. Baldwin-Lomax model is chosen to describe turbulence. A spatially-varying time-step and an implicit residual smoothing are used to accelerate convergence. A steady mixing approach is used to pass information between stator and rotor blades. For numerical optimization, searching direction is found by the steepest decent and conjugate direction methods, and the golden section method is used to determine optimum moving distance along the searching direction. The object of present optimization is to maximize efficiency. An optimum stacking line is found to design a custom-tailored 3-dimensional blade for maximum efficiency with the other parameters fixed.

Key Words : Numerical Optimization, Axial Compressor, Blade, Thin-Layer Navier-Stokes Equations, Stacking Line

1. Introduction

Turbomachines have complicated flow phenomena such as separation, turbulent wakes, secondary flows, and tip clearance vortices. Thus, accurate flow analysis is essential for designing efficient aerodynamic blade shapes that reduce loss. Recently, with the development of sophisticated measuring instruments and technology, precise measurement of turbomachinery flow fields are being obtained. This trend, coupled with rapid CFD development and the use of CFD in the design process, has led to the design of more efficient fluid machinery.

Within the past 15 years, research into the

design and use of shock free, controlled diffusion airfoils (CDA) for high-speed compressor applications have been successfully completed. The new designs use custom-tailored airfoils rather than the standard series of blade profiles such as NACA 400, NACA 65/circular arc, and double circular arc (Lakshminarayana, 1996). The CDA profiles minimize loss sources by diffusing the flow from supersonic to subsonic velocities without a shock wave, and by delaying boundary layer separation.

Hobbs and Weingold (1984) analytically developed a series of controlled diffusion airfoils to be shock-free and to avoid surface boundary layer separation. In experimental cascade testing, the CDA profile demonstrated the capability of achieving low loss and increased incidence range at elevated Mach numbers, high loading levels, and thicker leading and trailing edges, without performance penalty.

The CDA performance was compared with that of conventional NACA 65 airfoils by Rechter, et al (1985). Two alternative sets of stator blades

* Corresponding Author,

E-mail : kykim@inha.ac.kr

TEL : +82-32-872-3096 ; FAX : +82-32-868-1716

School of Mechanical, Aerospace and Automation Engineering, Inha University, 253 Yonghyun-dong, Nam-ku, Incheon 402-751, Korea. (Manuscript

Received February 15, 2000 ; Revised May 24, 2000)

were designed and built, each having the same design condition. Cascade and compressor tests, under the same flow conditions, revealed the superiority of the CDA profile for axial compressors over NACA 65 airfoils.

However, the capability of these modern airfoil profiles to realize their peak aerodynamic potential is limited by three-dimensional flow effects. This is a result of these technical advances being built on the basis of a two-dimensional compressible potential flow code combined with an improved boundary layer code. To design a full-span blade shape, Behlke (1986) used an integrated core/endwall vortex design model to apply CDA technology to the blade sections near the endwalls.

In this paper, optimization of the three-dimensional shape of a stator through the use of a single stage rotor-stator calculation is described. The flow field is treated as three-dimensional and viscous. The airfoil stacking line is chosen as the variable to be optimized. This line is difficult to optimize using conventional design methods. The airfoil stacking line is also an important variable in the determination of the 3-D blade shape.

2. Flow Analysis

Three-dimensional Navier-Stokes equations and energy equation are solved on body-fitted grids using an explicit finite-difference scheme. Viscous terms in the streamwise direction are neglected using a thin-layer approximation, and those in other directions are calculated. The Baldwin-Lomax model is chosen as the turbulence model. An explicit Runge-Kutta scheme is used to march from the initial to steady state with a spatially varying time step to accelerate convergence. Artificial dissipation terms are added to resolve shocks. Mach numbers in each direction, total pressure, and total temperature are given at the inlet. At the exit, the hub static pressure ratio is specified, and the radial equilibrium equation is solved along the blade span. A periodic tip clearance model is used to calculate rotor tip and stator hub tip clearance flows. A no-slip and an adiabatic wall conditions are used.

An H-type grid for the inlet flow region and C-type grids around the rotor and stator are used. Grids are overlapped by one cell at the interface between two adjacent grid blocks because of the node-centered finite-difference scheme used in the solver. At the interface, the solutions next to the boundary are integrated circumferentially at each spanwise location and then they are stored for use as boundary conditions for the neighboring grids.

3. Compressor Blade Design Approach

Although compressor blades are typically designed on stream surfaces, coordinates of blade sections are actually determined on a surface normal to the radial direction for the convenience of construction.

There are some general rules for compressor blade design. Diffusion rates on the blade surfaces should be reduced as much as possible. The three-dimensional blade shape must be consistent with the operating condition which varies along the span. In addition some aerodynamic characteristic variables must be insensitive over a wide operating range. As shown in the case of CDA airfoil shapes, efforts to reduce loss by controlling diffusion on the surface of a blade section have been relatively successful. However, these design methods have not been developed sufficiently to allow design of full-span blade shapes that satisfy the complicated three-dimensional flowfield in turbomachinery. Therefore, in this work, to take account for the effects of three-dimensional flow structure in the design, stacking line optimization of the stator was the main design objective.

The stacking line determines the relative circumferential coordinates of blades being stacked in the radial direction. A leaned and skewed blade can decrease the total energy loss through reduced secondary flow and diffusion in the blade passages. For example, in a turbine application, leaned, positively curved, and negatively curved blade cascades were tested experimentally by Han et al (1994). In the case of the negatively curved blade, the secondary vortical losses were greatly reduced, and the efficiency was raised. Similarly,

Chen (1995) analyzed the effects of turbine stator lean and skew on aerodynamics. Straight-leaned, sabre-shape, J-shape and S-shape turbine stators were analyzed using a three dimensional Navier-Stokes solver. The analysis suggested that the J-

shape had the highest total mass-averaged adiabatic efficiency. For a multistage compressor, Weingold, et al. (1997) designed a bowed stator through a three-dimensional Euler analysis. Experimental testing of the bowed stator in a

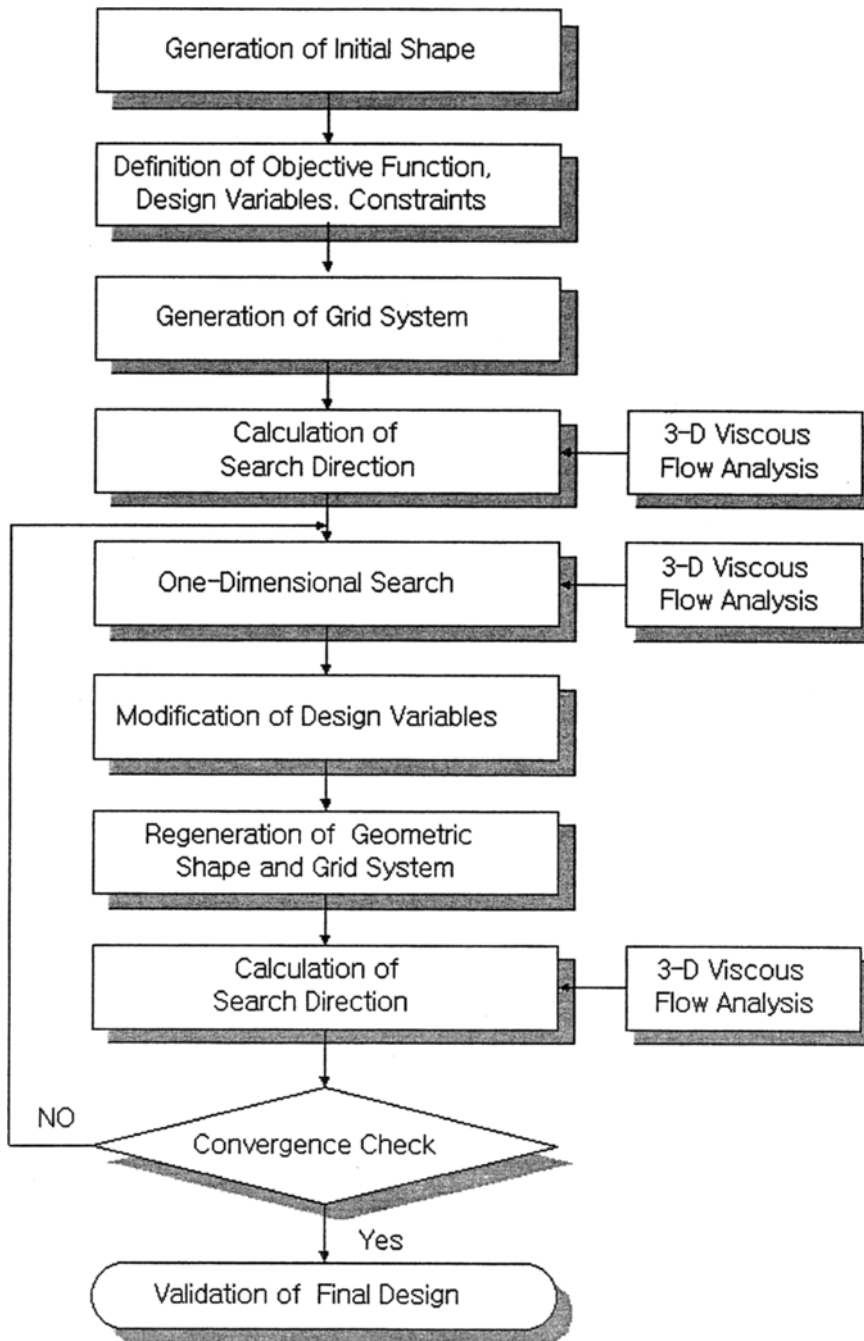


Fig. 1 Flow Chart of Optimization Process

three-stage research compressor confirmed the elimination of suction surface corner separation.

In this study, a single stage three-dimensional viscous flow analysis was conducted to reflect the interaction between the rotor and stator throughout the optimization process. The blade section is kept unchanged, and only the circumferential coordinates are modified by the stacking line. To formulate the stacking line, a second-order polynomial is used, and the polynomial is determined by three design variables; the values at 5%, 50%, and 95% span from the hub.

4. Numerical Optimization

The general numerical optimization problem is expressed as follows.

$$\text{Minimize } f(\mathbf{x}) \tag{1}$$

$$\text{Subject to } x_i^l < x_i < x_i^u \quad i=1, n \tag{2}$$

where, $f(\mathbf{x})$ is the objective function, and x_i^l, x_i^u, x_i are the lower and upper bounds of design variables, The search direction is initially found by the steepest decent method (Arora, 1989), and subsequently the conjugate direction method is used. The golden section method is used to determine the optimum moving distance along the search direction. The same optimization algorithms have been used to design an automotive cooling fan (Choi, et al., 1997). In gradient based optimization methods such as used in this work, the direction is calculated from the gradients of the objective function. Convergence criterion is also based on the norm of the gradient of the objective function. Figure 1 shows the flow chart of the optimization process.

Efficiency is chosen as the objective function. If the temperature rise is not large, the specific heat at constant pressure is nearly the same at the inlet and exit. Then, the objective function follows

$$f = 1 - \eta \tag{3}$$

where,

$$\eta = \left(\frac{P_{0exit}}{P_{0inlet}} \right)^{\frac{\gamma-1}{\gamma}} - 1 \frac{T_{0exit}}{T_{0inlet}} - 1$$

5. Results and Discussion

The first stage of the four-stage ATKOM compressor (Benade, 1991) (Fig. 2) designed by Noel Penny Turbines(NPT) was selected for validation of the optimization process. Table 1 describes the rotor and the stator of the first-stage of this compressor.

Both the rotor blade and the hub of stator rotate. At the inlet, the total temperature is 288.15 K, the total pressure is 101.3 kPa, and the Mach number at mid-height is 0.477. Inception of the shock wave around the leading edge of the rotor is shown in Fig. 3. Figure 2 shows a $50 \times 28 \times 50$ H-type grid at the inlet, and a $140 \times 41 \times 50$ C-type grid around the rotor, and a $130 \times 41 \times 50$ C-

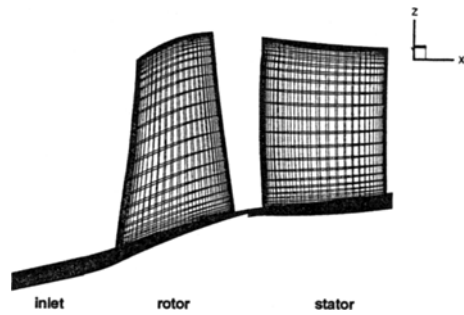


Fig. 2 Grid system for first stage rotor-stator of ATKOM compressor

Table 1 Rotor-stator geometry

	Blade number	Blade tip radius	Aspect ratio	Solidity
Rotor	34	132.2mm	1.47	1.9
Stator	37	132.2mm	1.34	1.77

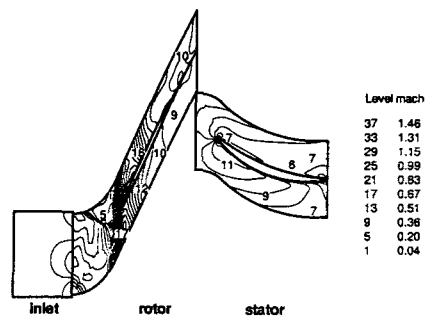


Fig. 3 Absolute Mach number contours (k=43)

Table 2 Results of the optimization

	OFV	Efficiency
Initial	0.23287	0.81548
Final	0.23118	0.82679

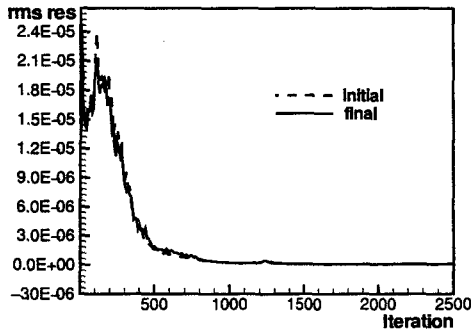


Fig. 4 History of root mean square residual (rms res)

type grid around the stator. The stacking line of original stator is almost straight.

Table 2 shows the results of optimization. Figure 4 shows the histories of root-mean-square residual (rms res) in flow calculations for initial and final shapes. These residuals are reduced by three orders to obtain the converged solutions. However, since the gradients of objective function are less sensitive to the residuals, the gradients, in the procedure of optimization, were obtained after the residual is reduced by only single order at relatively coarse grid system (95 × 36 × 40 C-type grid around rotor and stator) to save computing time. Thus, with these calculations, the values of the objective function rather than the gradients were not converged. This is the reason why the values of objective function are not consistent with the efficiency in the last column of Table 2, which were obtained from exact calculations. However, efficiency improvement at each iteration step was confirmed by the converged solution with the fine grids (Fig. 2). Finally, the stage efficiency was increased by 1.1 percent. Figure 5 shows the history of the objective function (F). After the eleventh iteration, the changes in the value become very small.

Optimizations were run on a personal computer with PENTIUM III 450 MHz processor. With the

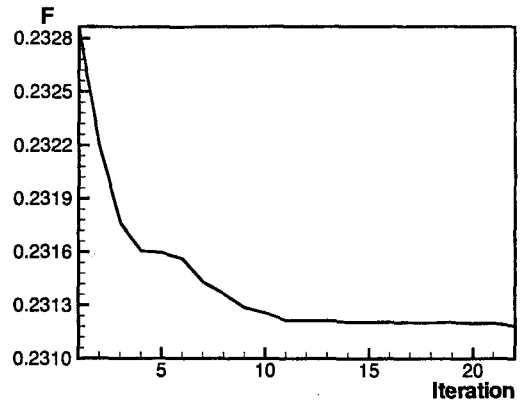


Fig. 5 History of objective function value

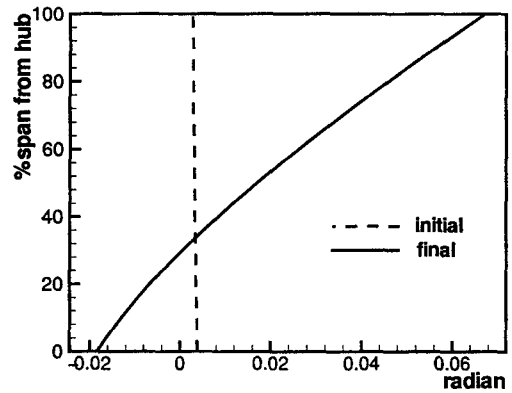


Fig. 6 Circumferential coordinates of stacking line after optimization

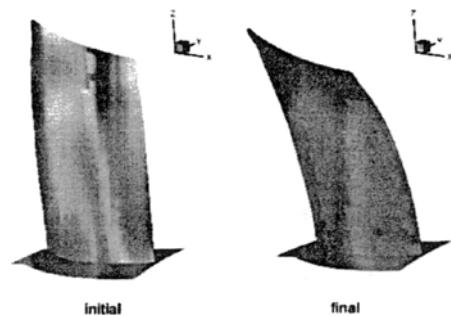


Fig. 7 Modification of stator shape after optimization

coarse grid system, it took 58 seconds to generate a grid system (stator grids are generated, and then, combined with rotor grids). Each flow calculation to obtain the gradient took about 44 minutes. Total number of flow calculations during the optimization process is 483.

Table 3 Mass-averaged quantities at the rotor exit

	Initial	Final
Absolute Mach number	0.53923	0.54151
Total pressure rise	1.53064	1.53404

Table 4 Mass-averaged quantities at the stator exit

	Initial	Final
Absolute Mach number	0.3887	0.3966
Total pressure rise	1.51701	1.52123

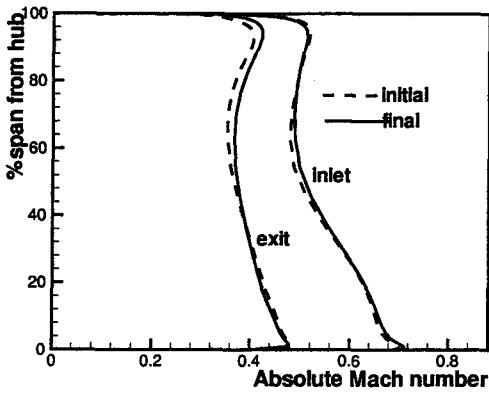


Fig. 8 Change of inlet and exit Mach numbers of stator

Figure 6 shows the modification of the stacking line, exaggerated circumferentially, after optimization. Figure 7 shows the corresponding change in the stator shape. The resulting stacking line is curved in the same direction as the referenced “bowed” stator. In addition, the stacking line is also leaned, with the upper part slightly more skewed than the lower part.

Single stage calculations changed the flow quantities at the rotor and stator exits. Mach numbers at rotor and stator exits are increased (Tables 3 and 4). Consequently, the mass flow rate is increased slightly. Efficiency based numerical optimization resulted in the increase of total pressure rise at the stator exit, and also at the rotor exit. Figure 8 shows the changes of inlet and exit Mach numbers of the stator in the spanwise direction.

Table 5 shows pressure and loss coefficients of the stator. The pressure loss coefficients decreased

Table 5 Pressure and loss coefficients of the stator

	Initial	Final
Pressure coefficient	0.40404	0.39040
Loss coefficient	0.04961	0.04602

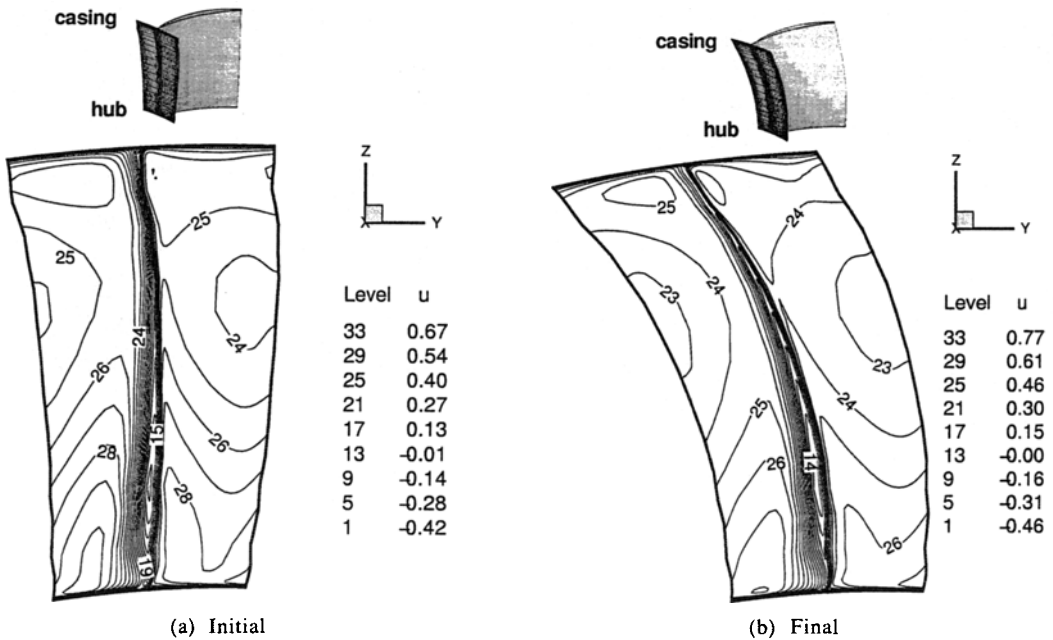


Fig. 9 Absolute axial Mach number contours at stator exit

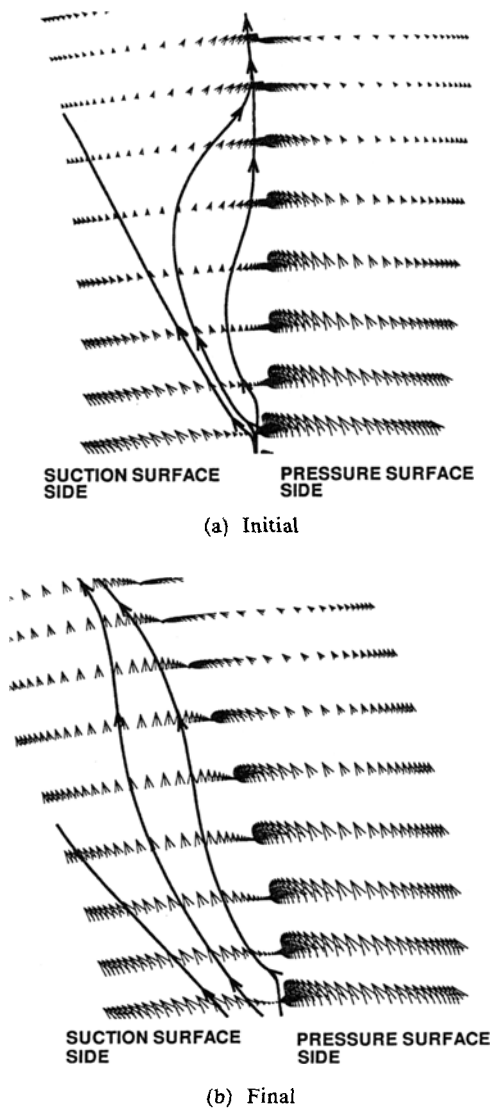


Fig. 10 Absolute velocity vectors on the upper part of stator exit

as a result of the optimization. Massardo et al (1990) show that the increase in efficiency can be accompanied by negative influence on other important variables; weight of stage, stall margin, etc. Therefore, to improve the overall performance, the use of multivariable objective function can be considered.

Changes in the flowfield, due to the modification of stacking line, is remarkable. Figure 9 shows axial Mach number contours at the exits of the initial and optimized stators, respectively. The

effect of the wake (one of the dominant losses) near the casing is found to be decreased. Also, the axial Mach number is increased at mid span. Consequently, the secondary flow and loss are decreased.

Figure 10(a) shows the absolute velocity vectors on the upper part of the exit plane of the initial stator. The mixing of wakes produces large outward radial velocities and streamlines toward the wakes. However, the flowfield after optimization (Fig. 10(b)) shows relatively uniform velocity vectors. The mixing of wakes is suppressed by varying the circumferential locations where wakes are originated, in radial direction.

Compressors have to allow wide flow variations along the performance curve. In this study, however, no attempt has been made to optimize the overall operating range. It is left as a future work.

6. Conclusion

Through a single stage viscous flow analysis, the stator shape for an existing compressor stage is optimized numerically. An efficiency-based objective function is minimized by varying the stacking line, for a given blade section. As a result, the efficiency is increased by 1.1 percent. The total pressure rise across both rotor and stator are increased. The flowfield at the stator exit shows that the effect of wakes is suppressed.

Acknowledgements

The authors wish to acknowledge the financial support of the Korea Research Foundation made in the Program Year 1996.

References

- Arora, J. S., 1989, *Introduction to Optimum Design*, McGraw-Hill
- Behlke, R. F., 1986, "The Development of a Second Generation of Controlled Diffusion Airfoils for Multistage Compressors," *Journal of Turbomachinery*, Vol. 108, pp. 32~41.
- Benade, G., 1991, *Aerodynamic Design Report*

for the Four Stage Compressor, Noel Penny Turbines Company.

Chen, N., 1995, "A Comparative Study on Different Leaned and Skewed Bladings in a Turbine Stator by 3-D Navier-Stokes Analysis," AIAA 95~2189.

Choi, J. H., Kim, K. Y., and Chung, D. S., 1997, "Numerical Optimization for Design of an Automotive Cooling Fan," *Journal of Passenger Cars*, Vol. 106, pp. 1485~1489.

Han, W., Wang, Z., Tan, C., Shi, H., and Zhou, M., 1994, "Effects of Leaning and Curving of Blades With High Turning Angles on the Aerodynamic Characteristics of Turbine Rectangular Cascades," *Journal of Turbomachinery*, Vol. 116, pp. 417~424.

Hobbs, D. E. and Weingold, H. D., 1984, "Development of Controlled Diffusion Airfoils for Multistage Compressor Application," *Journal of Engineering for Gas Turbines and Power*, Vol. 106, pp. 271~278.

Lakshminarayana, B., 1996, *Fluid Dynamics and Heat Transfer of Turbomachinery*, John Wiley & Sons Inc.

Massardo, A., Satta, A., and Marini, M., 1990, "Axial Flow Compressor Design Optimization : Part 1 Pitchline Analysis and Multivariable Objective Function Influence," *Journal of Turbomachinery*, Vol. 112, pp. 399~404.

Rechter, H., Steinert, W., and Lehmann, K., 1985, "Comparison of Controlled Diffusion Airfoils With Conventional NACA 65 Airfoils Developed for Stator Blade Application in a Multistage Axial Compressor," *Journal of Engineering for Gas Turbines and Power*, Vol. 107, pp. 494~498.

Weingold, H. D., Neubert, R. J., Behlke, R. F., and Potter, G. E., 1997, "Bowed Stators: An Example of CFD Applied to Improve Multistage Compressor Efficiency," *Journal of Turbomachinery*, Vol. 119, pp. 161~168.